Instability-induced hierarchy in bipedal locomotion

Kunishige Ohgane*
National Center for Geriatrics and Gerontology, Obu, Aichi 474-8511, Japan

Kei-Ichi Ueda
Research Institute for Mathematical Sciences, Kyoto University, Kyoto 606-8502, Japan

(Received 2 June 2007; revised manuscript received 25 February 2008; published 19 May 2008)

One of the important features of human locomotion is its instant adaptability to various unpredictable changes of physical and environmental conditions. This property is known as flexibility. Modeling the bipedal locomotion system, we show that *initial-state* coordination by a *global variable* which encodes the attractor basins of the system can yield flexibility. This model is based on the following hypotheses: (i) the walking velocity is a global variable, and (ii) the leg posture at the beginning of the stance phase is the initial state of the gait. Moreover, we confirm these hypotheses. We investigate the regions near the neutral states between walking and falling phases using numerical experiments and demonstrate that global variables can be defined as the dominant unstable directions of the system dynamics near the neutral states. We propose the concept of an "instability-induced hierarchy." In this hierarchy, global variables govern other variables near neutral states; i.e., they become elements of a higher level.

DOI: 10.1103/PhysRevE.77.051915 PACS number(s): 87.19.ru, 87.19.L−, 87.16.A−

I. INTRODUCTION

An important feature of human locomotion is its instant adaptability to unpredictable changes of various conditions affecting locomotion. Indeed, walking is robust to not only environmental changes (e.g., wind), but also physical changes (e.g., impairment due to injury). If anything, these perturbations result in a modified walking pattern, although such changes can sometimes be dramatic. The mechanisms underlying such flexible control are of interest to scholars in neuroscience, biomechanics, and physical sciences [1–3]. This study is directed toward gaining a theoretical understanding of the mechanisms of flexible locomotor control in the presence of various condition changes.

Modeling studies of bipedal locomotion [4,3] based on neurophysiological evidence have shown that a basic walking gait is generated through mutual entrainment between oscillations of a central pattern generator (CPG) [5] and the body itself. A human locomotor CPG has been identified in the spinal cord [6,7]. A walking pattern is formed as a limit cycle in phase space, and the robustness of walking patterns can be attributed to the stability of the corresponding limit cycle. It is reasonable to suppose that the formation of walking patterns in a flexible manner can be facilitated by the flexibility of the limit-cycle attractor to changes.

Theoretical studies of dynamical systems [8–10] have demonstrated that in the neighborhood of the neutral state (the unstable region between stationary and periodic solutions), even a slight difference in the way the system approaches the neutral state can separate the system to converge to quite different behaviors. Modeling based studies of human gait generation [11,12] have suggested that the neutral state is latent in the walking system—i.e., in the coupled system composed of the CPG and the body—and can surface as the leg posture at the beginning of the stance phase (BSP) according to perturbations. From a biomechanical perspective, as shown in Fig. 1, the joint angle of the hip, ϕ_h, and knee, ϕ_k, at the BSP can make neutral states surface states and determine the subsequent behavior of the system. Indeed, neurophysiological experiments on animal locomotion show that walking overcomes perturbations through modulation of the leg posture at the BSP [13–18].

The initial state is one of the constraints because it determines the time evolution of the system. Since the leg posture at the BSP determines the subsequent behavior of the walking system—i.e., whether the system continues to walk or not—it may be natural to describe it as the *initial state*. Thus, from the viewpoint of neurophysiology and dynamical sys-

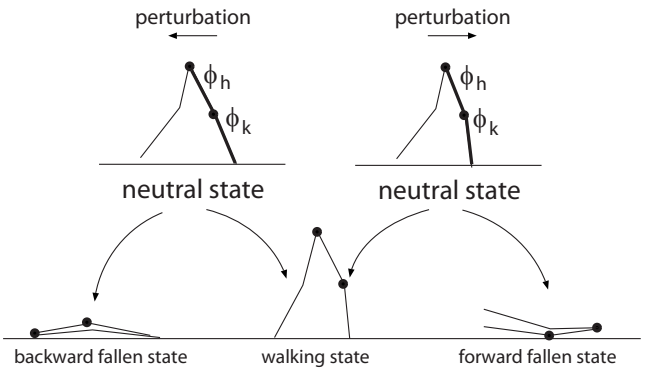

FIG. 1. A biomechanical view of bipedal walking. The leg posture is determined by the hip and knee joint angles—i.e., ϕ_h and ϕ_k. The behavior of the walking system is separated into three states: forward fallen, walking, and backward fallen. The neutral states exist between the two adjacent states—i.e., between the forward fallen and walking states and between the walking and the backward fallen states. Depending on perturbations, the neutral state can surface as the leg posture—i.e., ϕ_h and ϕ_k. The two neutral states separate the behavior of the system into the forward fallen and walking states and the walking and backward fallen states.

*ohgane@nils.go.jp

tems theory, posture modulation at the BSP is crucial for maintenance of walking.

Modeling studies [11,12] have predicted that initial-state coordination can reproduce adaptive pattern formation for walking. However, in their models, adaptability to any perturbations is low because only the knee joint angle ϕ_k was coordinated as the initial state. Moreover, above all, only adaptability specific to each perturbation can be reproduced because the initial-state coordination is formulated according to the perturbation.

In this article, we emphasize that flexibility can be established by governing the initial state with the whole state of the system. Undoubtedly, any perturbation such as a change in the body or an external force is reflected in the whole state of the walking system. Therefore, if the equation of the initial-state coordination is given appropriately, as a function of the variable coding the whole state, such a model will adapt to changes in various conditions. From a mathematical viewpoint, coding the whole state is equivalent to coding the attractor basins of the system. We regard a variable which can encode the attractor basins of the walking system as a *global variable*.

In Sec. II, we propose a model as an extended version of the models [11,12] by adding modulation of the hip joint angle ϕ_h to the initial-state coordination. In Sec. III, hypotheses (i) and (ii) below are demonstrated through numerical experiments in the neighborhood of the neutral states (just before the BSP).

(i) There exists a global variable in bipedal walking systems.

(ii) The posture at the BSP is the initial state.

Based on numerical experiments, we formulate the equations of initial-state coordination by a global variable in Sec. IV. Since this model is described by only the variables of the system, adaptability to various perturbations may be obtained autonomously regardless of the kind of perturbation, without specific control for each perturbation. In Sec. V, we demonstrate that a global-variable-coordinated initial state establishes flexibility. Since the global variable representing the behavior of the whole system governs the other variables expressing the behavior of the body parts, the global variable is on a different hierarchical level from other variables. This coordination demonstrates the interaction between two hierarchical levels. Flexibility, which is an essential characteristic of biological creatures, is thus yielded by such a hierarchy. We also propose a concept of hierarchy called *instability-induced hierarchy*, and it can be defined only in the neighborhood of the neutral states as global dominance in a system. This hierarchy is different from a master-slave relationship, such as the slaving principle [19], in which dominant variables govern a system also in stable states.

II. MODEL

We use a simple neurobody walking system to demonstrate the hypotheses proposed in Sec. I. The walking model should also provide the framework to design a model of flexible locomotor control. The structure of the model employed is basically the same as that presented in [12], but the model differs in the following respect. The leg posture attribute is extended to include the angle of the hip joint in addition to the angle of the knee joint. We consider that these two (hip and knee) joints are important to form adaptive walking patterns.

The model was constructed simply from a theoretical perspective by adding only the posture controller (PC) to the coupled system composed of a CPG and a body. The model thus consists of the body and a neural system composed of a CPG and a PC, as shown in Fig. 2.

The body consists of an interconnected chain of five rigid links in the sagittal plane, as shown in Fig. 2. The motion of the body is represented by differential equations of a vector $\mathbf{x}=(x_1,\ldots,x_6)$ describing five links (cf. Fig. 2)—i.e., the mass point position of one link and inertial angles for four links. (x_1,x_2) represents the position of the hip joint, x_3 and x_4 (x_5 and x_6) represent the angles of the left (right) shank and thigh with respect to the vertical, respectively. The equations are expressed according to the Newton-Euler method.

The CPG and PC are composed of 12 (from the 1st to the 12th neurons) and 4 neurons (from the 13th to the 16th neurons), respectively. The essential function of each neuron is to cause an action potential over a particular interval in each phase. The interval of the action potential is determined by the frequency of the corresponding neuron. The phase at which the action potential of a neuron occurs is determined by the connectivity of the neural system.

The neural system has both excitatory and inhibitory connections. The excitatory and inhibitory connections between the neurons can make the relative phase of neuronal activity synchronous or opposite, respectively. Each neuron in the CPG and PC induces a torque at a specific joint and an angle-modulating torque at the hip and knee joints, respectively. The equations describing the neural system are written in Appendix A.

The coupled system composed of the CPG and body generates a basic gait. To modify the basic gait, the PC modulates the leg posture around the BSP which is determined by the hip and knee joint angles. This modulation is executed by assigning the equilibrium angles ϕ_h and ϕ_k to the hip and knee joints, respectively, while the neuron of the posture controller is firing. The hip PC neurons u_{13} and u_{14} govern the modulation of the angles of the hip joints in the left and right legs, respectively. The knee PC neurons u_{15} and u_{16} govern the modulation of the knee joint angles of the left and right legs, respectively. Being entrained by the CPG activity, each hip PC neuron outputs its action potential in the swing phase. Each knee PC neuron outputs its action potential around each BSP [12] (see the last paragraph in this section). The equilibrium angles produce the following posture modulating torques at the hip joint (T_{BSPlh},T_{BSPrh}) and the knee joint (T_{BSPlk},T_{BSPrk}): i.e., $\mathbf{T}_{BSP}=(T_{BSPlh},T_{BSPlk},T_{BSPrh},T_{BSPrk})$. They are defined as follows:

$$T_{BSPlh}=f_m(T_{lh}-\beta_h f(u_{13});\delta_h),$$

$$T_{BSPrh}=f_m(T_{rh}-\beta_h f(u_{14});\delta_h),$$

$$T_{BSPlk}=f_m(T_{lk}-\beta_k f(u_{15});\delta_k),$$

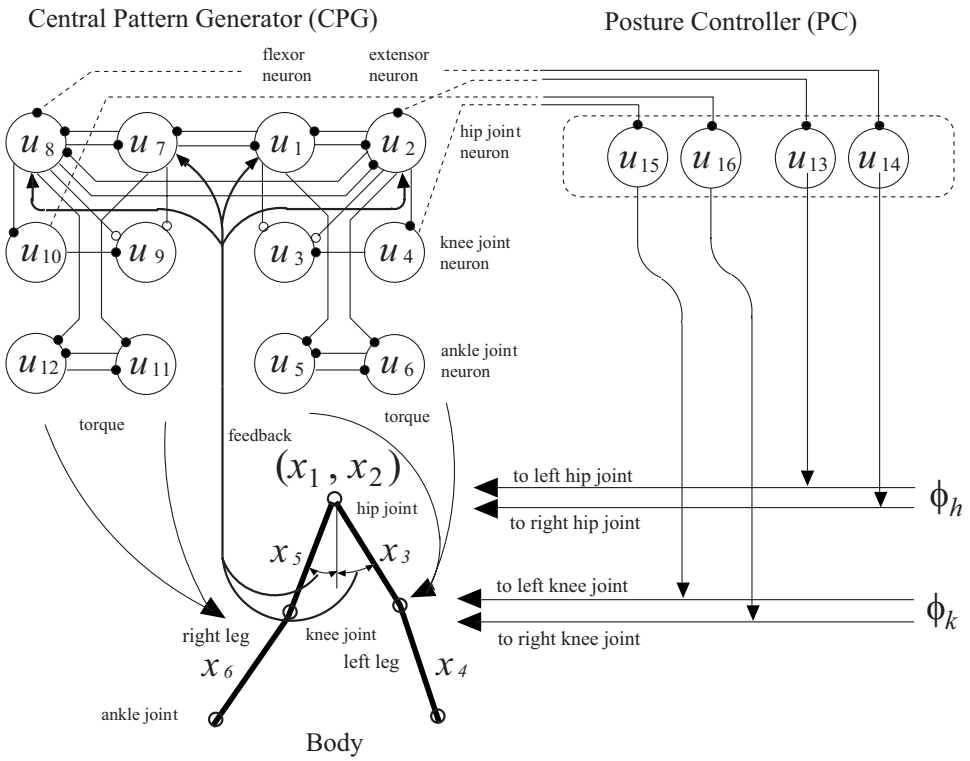

FIG. 2. The walking model consists of the posture controller (PC; neurons 13–16) and a coupled system composed of the central pattern generator (CPG; neurons 1–12) and the body. ○ and ● denote excitatory and inhibitory connections, respectively. The motion of the hip, knee, and ankle joints in the left leg is governed by neurons 1-2-13, 3-4-15, and 5-6, respectively. Similarly, the motion of the joints in the right leg is governed by neurons 7–12, 14, and 16. Odd-numbered neurons and even-numbered neurons in the CPG control joint flection and posture, respectively. Given the equilibrium angles ϕ_h and ϕ_k, the PC modulates the angles of the hip and knee joints, respectively, at the BSP.

$$T_{BSPrk} = f_m(T_{rk} - \beta_k f(u_{16}); \delta_k),$$

$$T_{lh} = g(u_{13}) f(x_3 - x_5 - \phi_h)[p_{h1}(x_3 - x_5 - \phi_h) - p_{h2}(\dot{x}_3 - \dot{x}_5)],$$

$$T_{rh} = g(u_{14}) f(x_5 - x_3 - \phi_h)[p_{h1}(x_5 - x_3 - \phi_h) - p_{h2}(\dot{x}_5 - \dot{x}_3)],$$

$$T_{lk} = g(u_{15}) f(x_3 - x_4 - \phi_k)[p_{k1}(x_3 - x_4 - \phi_k) - p_{k2}(\dot{x}_3 - \dot{x}_4)],$$

$$T_{rk} = g(u_{16}) f(x_5 - x_6 - \phi_k)[p_{k1}(x_5 - x_6 - \phi_k) - p_{k2}(\dot{x}_5 - \dot{x}_6)],$$

$$f(u) = \max(0, u),$$

$$f_m(z; \delta) = \begin{cases} \delta & \text{for } z > \delta, \\ z & \text{for } |z| \le \delta, \\ -\delta & \text{for } z < -\delta, \end{cases}$$

$$g(z) = \begin{cases} 0 & \text{for } z \le 0, \\ 1 & \text{otherwise}, \end{cases} \tag{1}$$

where $x_3 - x_5$ and $x_5 - x_3$ represent the angle of the left and right hip joints, respectively; $x_3 - x_4$ and $x_5 - x_6$ represent the angle of the left and right knee joints, respectively; ϕ_h, ϕ_k, δ_h, δ_k, β, p_{h1}, p_{h2}, p_{k1}, and p_{k2} are constant coefficients. Since $-\beta_h f(u_{13})$, $-\beta_h f(u_{14})$, $-\beta_k f(u_{15})$, and $-\beta_k f(u_{16})$ function antagonistically with respect to T_{lh}, T_{rh}, T_{kh}, and T_{kr}, respectively, the joint angles are forced to approach the equilibrium angles during PC neuron firing. $f_m(z; \delta)$ is a function which restricts the torque amplitude to a realistic level [20] necessary to maintain a walking movement. The function $f_m(z; \delta)$ may be realized through the coactivation of the agonists and antagonists at the joint.

The PC receives the sensory signal encoding the output of the CPG and governs the leg posture around the BSP. Purkinje cells in the cerebellum also receive proprioceptive sensory signals and outputs from the CPG [21,22]. Purkinje cells in the cerebellum strongly participate in the moderation of the leg posture at the BSP. Neurophysiological experiments on animal locomotion [15] show that the groups of Purkinje cells which affect parts of the limb exist in lobule V of the paravermal part of the cerebellum. The activities of the Purkinje cell groups affecting the proximal part and the elbow-related part peak in the swing phase and around the BSP of the limb, respectively. Based on this knowledge, the hip and knee PC neurons in our model were designed to produce their action potentials in the swing phase and around the BSP, respectively (Fig. 3). Such a phase relationship in the firing of the PC neurons realizes an effective modulation of the leg posture in computer simulations.

Given an appropriate initial condition, the proposed model (1) generates a walking behavior, which approaches a quasiperiodic orbit. Figure 3 demonstrates an example walking trajectory of the system; the profile of the walking velocity $\dot{x}_1$ which is the velocity of the hip joint position on the horizontal axis, the thigh angle x_3, the knee joint angle $x_3 - x_4$, and firing pattern of u_{13} and u_{15} are shown. The walking velocity fluctuates between 0.9 and 1.4 m/s within one period, and it reaches the maximum value at the BSP and the minimum value near the midpoints between the BSPs. The knee joint angle peaks to 0.8 rad near the midpoints of the swing phase and reaches the minimum value 0 rad near the BSP. The thigh angle x_3 peaks at a little before the BSPs and reaches the minimum value near the midpoints between the BSP. These agree with data shown in biomechanical studies [23,24]. The motion range of the thigh angle x_3 is approxi-

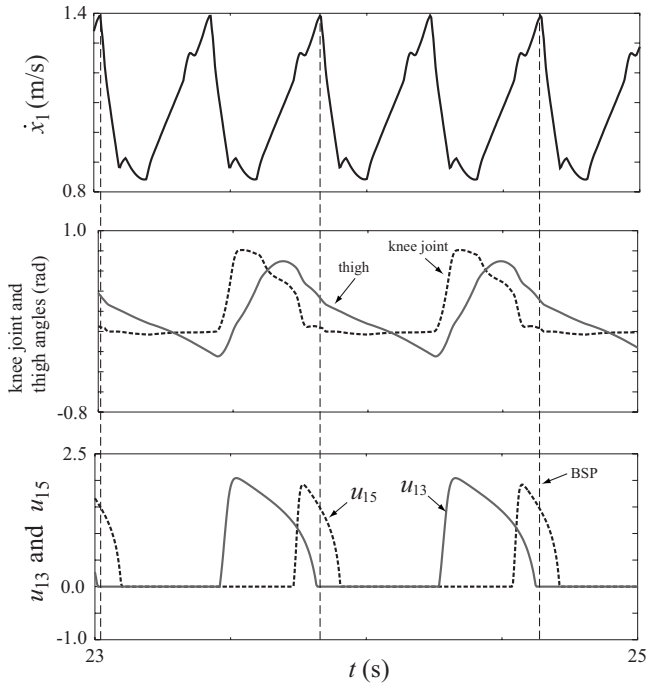

FIG. 3. The profile of $\dot{x}_1$ (top), thigh angle x_3 (gray line in center), knee joint angle x_3-x_4 (dashed line in center), u_{13} (gray line at the bottom), and u_{15} (dashed line at the bottom). Vertical dashed lines indicate the timing of the BSP of the left leg. u_{13} is active in the swing phase just before BSP and u_{15} is active around the BSP, which accords with neurophysiolosical knowledge [15]. T_{BSPlh} and T_{BSPlk} are produced only during firing of u_{13} and u_{15}, respectively.

mately $-0.2-0.7$ rad and has a difference of about $+0.1$ rad from the biomechanical results.

III. NUMERICAL EXPERIMENTS

The model has three qualitatively different phases—i.e., walking, falling forward, and falling backward—according to appropriate parameters and initial conditions. There exist neutral states between the falling and walking phases. Controlling the initial conditions, which are specified as the joint angles in the initial posture θ_{in} (see Appendix B 3), the neutral states can be observed despite the instability of such states. We first confirm numerically that neutral states are quasiperiodic solutions and have one dominant unstable direction in the dynamics of the system near the neutral states. We define global variables as variables with such unstable directions. The walking velocity is shown to be a global variable. Indeed, this variable completely represents the whole state of the system—i.e., which attractor basin the system is in. Therefore, control of this variable will yield the governing of the whole state. Next, we investigate how global variables can be controlled through the modulation of other variables—i.e., by posture control at the BSP.

A. Global variables

The second-order equation (A1) can be transformed to a 12-component first-order equation by introducing the variables $z_i=\dot{x}_i$. We ignore x_1, since the right sides of (A1) and $P(\mathbf{x})$ are independent of x_1.

We thus focus on the dynamics of the variables of the body $\tilde{X}=(x_2,\ldots,x_6,z_1,\ldots,z_6)\in\mathbb{R}^{11}$. Note that z_1 corresponds to the walking velocity. In the walking regime, solution orbits seem to approach stable quasiperiodic solutions. In fact, the maximum velocity occurring during every step of stable walking only varies within about 1% [Fig. 4(a)].

We demonstrate that the two neutral states are quasiperiodic orbits. The joint angle in the initial posture θ_{in} is taken as a bifurcation parameter. When θ_{in} is large enough, the body falls backward. When θ_{in} is decreased to $-0.019\,321\,1\pi$, subsequent walking is observed. As θ_{in} is further decreased to $-0.036\,954\,4\pi$, the body falls forward. Subsequent walking is thus observed between these transient points. By carefully tracing the orbital behavior near the transition points, it was found that the orbit approaches a quasiperiodic orbit for a while, before the system approaches a final state. Figure 4 shows the orbital behavior near the transition point. There are thus two neutral states between walking and falling, which we denote NF for the region between walking and falling forward, and NB for that of backward falling.

Since neutral states are unstable, orbits near neutral states move along unstable manifolds. We show that a one-dimensional unstable direction exists in $\tilde{X}$ which separates the final states of orbits at the neutral states for any gait phase. In order to confirm this direction, we performed careful numerical experiments on the system's behavior on the unstable manifold. We observed solution responses to small perturbations at the neutral states. Although perturbations to variables in the velocity dimension z_i can preserve the restricted conditions of the body structure, perturbations in the displacement dimension x_j break the restrictions by forcing the leg length to change. Thus, as a perturbation, we imposed a small extra force

$$\mathbf{F}=(0,\ldots,0,\underbrace{F_k}_{k},0,\ldots,0)\quad(k=1,\ldots,6)$$

(see Appendix A) to z_j for 0.1 ms in each gait phase. As shown in Fig. 5, the responses to perturbations indicate that the sign of F_1 is coherently responsible for the fate of the orbit in any gait phase. On the other hand, the response of the system to perturbations affecting $k=2,\ldots,6$ changes depending on the gait phase in which the extra force is applied. Moreover, for F_j $(j=2,\ldots,6)$, there exist refractory regions in which the system does not change its response for small perturbations. These numerical experiments strongly suggest that z_1 determines the final state of the system. It is reasonable to suppose that the z_1 axis corresponds to the dominant unstable direction in $\tilde{X}$ near the neutral states.

In order to confirm this hypothesis, we performed numerical experiments in which z_i was slightly perturbed for 0.1 ms by $\tilde{\mathbf{F}}=(F_1,\ldots,F_6)$. One thousand samples of combinations of F_j $(j=1,\ldots,6)$ were tested for each gait phase. F_1 was fixed at $+0.2$ for NB and -0.2 for NF, and F_j $(j=2,\ldots,6)$ were randomly chosen satisfying $\sqrt{F_2^2+\cdots+F_6^2}=0.2$ for each

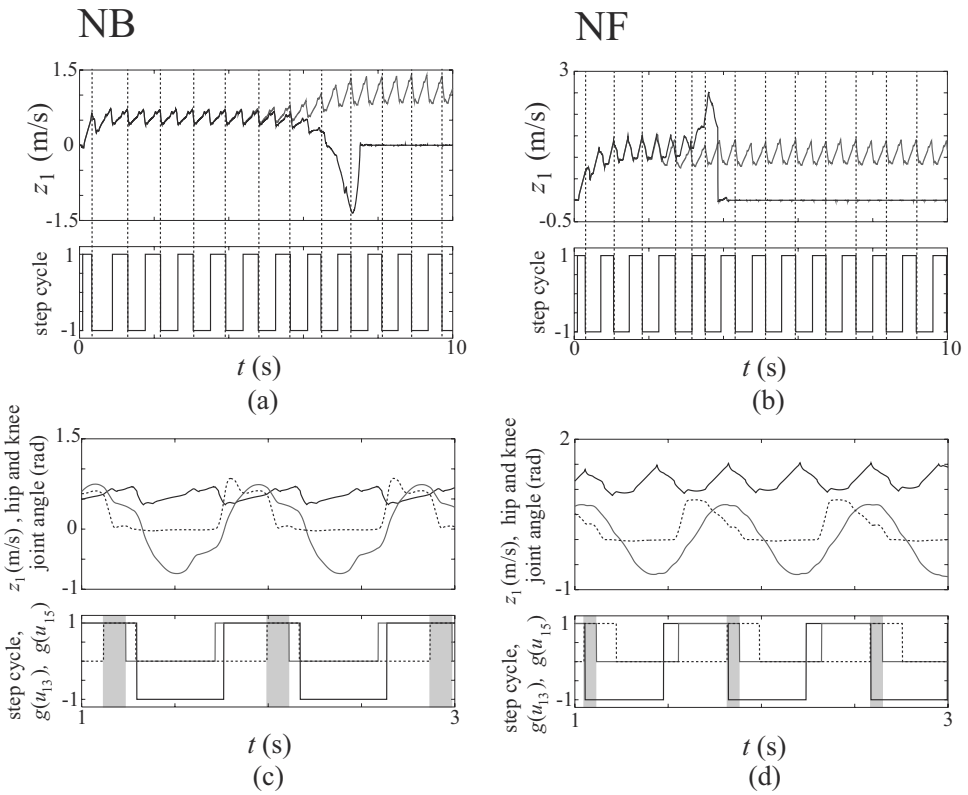

FIG. 4. (a) Upper: time series of z_1 for a bifurcation parameter near the neutral state NB. Solid and gray lines indicate the motion of z_1 when the system is started from the initial conditions (bifurcation parameter) $\theta_{in}=-0.0193211\pi$ and $\theta_{in}=-0.0193212\pi$, respectively. It can be seen that the orbits approach a quasiperiodic orbit for a while, before the system approaches the stable quasiperiodic orbit (subsequent walking) for $\theta_{in}=-0.0193212\pi$ (gray line), but instead enters the falling state for $\theta_{in}=-0.0193211\pi$ (solid line). (a) Bottom: solid line indicates the time series of the step cycle where the values 1 and −1 indicate the swing and stance phases, respectively. Vertical dashed lines indicate the timing of the BSP of the left leg. (b) Time series of z_1 for $\theta_{in}=-0.0369544\pi$ (solid line) and $\theta_{in}=-0.0369543\pi$ (gray line). The remaining notation is the same as in (a). (c) upper [(d), upper]: Magnified views of (a) [(b)]. Solid lines indicate the motion of z_1 for $\theta_{in}=-0.0193211\pi$ [$\theta_{in}=-0.0369544\pi$]. Gray and dashed lines indicate joint angle motion in the hip, x_3-x_5, and knee, x_3-x_4, respectively. (c) Bottom [(d), bottom]: solid line shows the time series of the step cycle. Gray and dashed lines indicate $g(u_{13})$ and $g(u_{15})$—i.e., the activities of the posture modulating torques at the hip T_{lh} and knee T_{lk}, respectively (1 and −1 indicate the active and nonactive phases, respectively). Gray rectangles indicate time intervals in which both T_{lh} and T_{lk} are active.

sample. As a result, we found that all of the samples induce the system to be attracted into the walking state for any gait phase. This indicates that F_j $(j=2,\ldots,6)$ hardly affect the final state of the system near the neutral states for any gait phase. That is, positive and negative perturbations to z_1 can make the system recover its walking near NB and NF, respectively. This means that the z_1 axis is almost parallel to the unstable direction which dominates the dynamics of the system near the neutral states (Fig. 6).

We remark that if neutral states are periodic solutions, then the dominant unstable direction can be confirmed by solving eigenvalue problems corresponding to the periodic orbits.

These numerical experiments demonstrate that z_1 is a global variable which encodes the attractor basins of the walking system. Critical values Z_b and Z_f exist for the walking velocity such that the system belongs to the walking state as long as $z_1>Z_b$ near NB and $z_1<Z_f$ near NF.

B. Posture modulation near neutral states

As demonstrated in the previous subsection, the global variable z_1 encodes the attractor basins. Control of this global variable will therefore govern the system so that it may be attracted toward a particular attractor basin. In this subsection, we investigate appropriate posture modulation controlling the global variable z_1. The walking system implements posture modulation around the BSP by giving the equilibrium angles ϕ_h and ϕ_k. The torque of the posture modulation at the hip and knee joints is active around the BSP, as shown in Figs. 4(c) and 4(d). In the neighborhood of NF, T_{lh} and T_{lk} are active simultaneously around the BSP. In the neighborhood of NB, on the other hand, T_{lh} and T_{lk} are active simultaneously just before the BSP.

We first show that the system can control z_1 by modulating leg posture around the BSP. Figure 7 shows an example. Modulation of ϕ_h just before the BSP allows z_1 to be controlled at the BSP. Furthermore, it is shown that controlling z_1 can determine whether or not the system is attracted to the walking state.

Next, in order to find appropriate posture modulation in $\phi_h-\phi_k$ space near the neutral states, we add small values $\delta\phi_h$ and $\delta\phi_k$ to ϕ_h and ϕ_k, respectively, during the active phase of torque modulation at the hip and knee joints. The values are chosen such that $(\phi_h,\phi_k)=(\bar{\phi}_h+\delta\phi_h,\bar{\phi}_k+\delta\phi_k)$ for

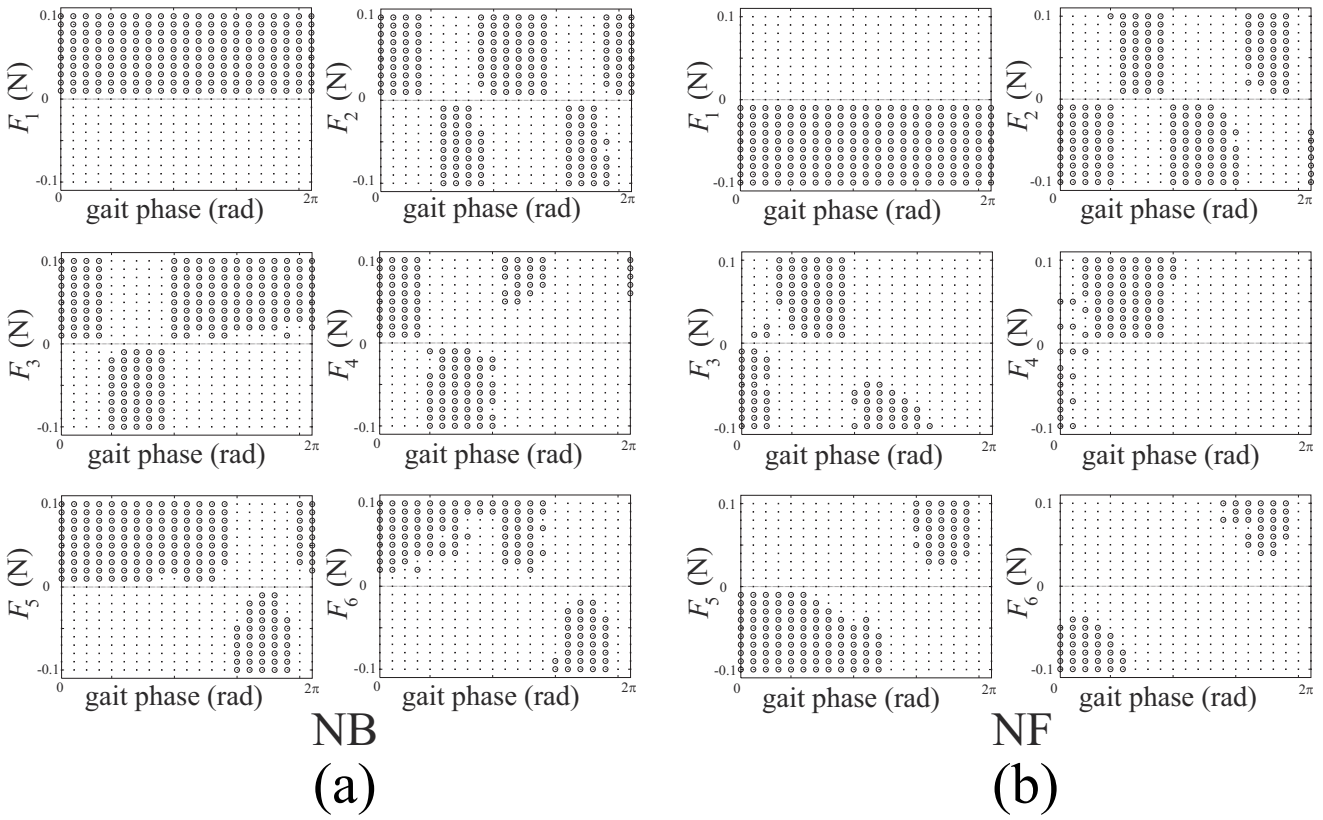

FIG. 5. (a) [(b)] Response of the system to a perturbation of F_j near NB [NF]. White circles [black dots] indicate the values of the parameters for which the system is attracted to the walking state [falling state]. The horizontal axis denotes the gait phase in which perturbation is applied. The vertical axis denotes the amplitude of perturbation F_j. The responses are sensitive to small perturbations in F_1 and determined for each phase by the sign of F_1.

$t \geq t_0$, where $\delta\phi_h$ and $\delta\phi_k$ are chosen satisfying $\sqrt{(\delta\phi_h)^2+(\delta\phi_k)^2}=\epsilon(\epsilon\in[0.001,0.01])$ and t_0 is chosen during the active phase of torque modulation at the hip and knee joints. Figure 8 shows the distribution of the system's final state induced by a combination of $\delta\phi_h$ and $\delta\phi_k$. The system can be attracted to the walking state for any gait phase by taking $(\delta\phi_h, \delta\phi_k)$ from the upper-left region of Fig. 8(a) near NB and from the right region of Fig. 8(b) near NF. Furthermore, the distribution does not qualitatively change at t_0—i.e., just before the BSP. This means that the BSP is an initial state constraining the dynamics of the system.

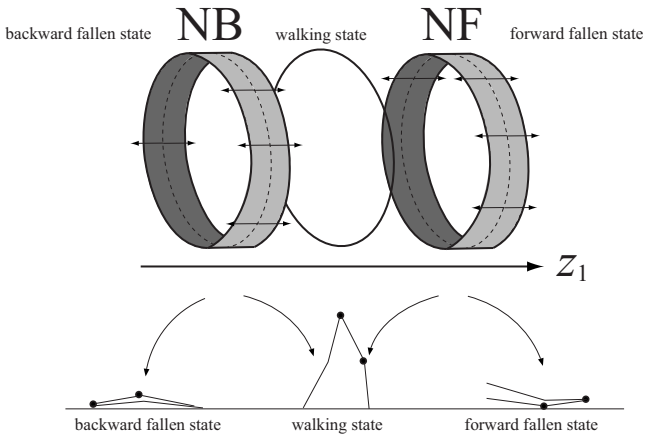

FIG. 6. Schematic figure of the system's phase space. Horizontal arrows emanating from NB and NF indicate the dominant unstable directions corresponding to the axes of the global variable.

IV. INTERACTION BETWEEN THE GLOBAL VARIABLE AND OTHER VARIABLES

We show that initial-state coordination according to the global variable improves adaptability to various perturbations. As mentioned in Sec. III, z_1 is a global variable which encodes the attractor basins and the posture at the BSP is the initial state of the system. We thus describe the initial state as a function of the global variable. We take Φ_h and Φ_k, which are functions of z_1, as substitutes for ϕ_k and ϕ_k.

The numerical experiments in Sec. III B lead to the design of equations for adaptive coordination functions determined as

$$\Phi_h(z_1) = \bar{\phi}_h + \alpha_{hf} f(z_1 - z_f) + \alpha_{hb} f(z_b - z_1), \tag{2a}$$

$$\Phi_k(z_1) = \bar{\phi}_k + \alpha_{kb} f(z_b - z_1), \tag{2b}$$

where z_b, z_f, α_{hf}, α_{hb}, and α_{kb} are constants. In Sec. III, we found a threshold for the walking velocity. That is, the walking system belongs to the side of the attractor basins when $z_1 \geq Z_b$ near NB and $z_1 \leq Z_f$ near NF where $Z_b \approx 0.4$ m/s and $Z_f \approx 1.5$ m/s. When $z_1 < Z_b$ or $z_1 > Z_f$, Φ_h and Φ_k should be

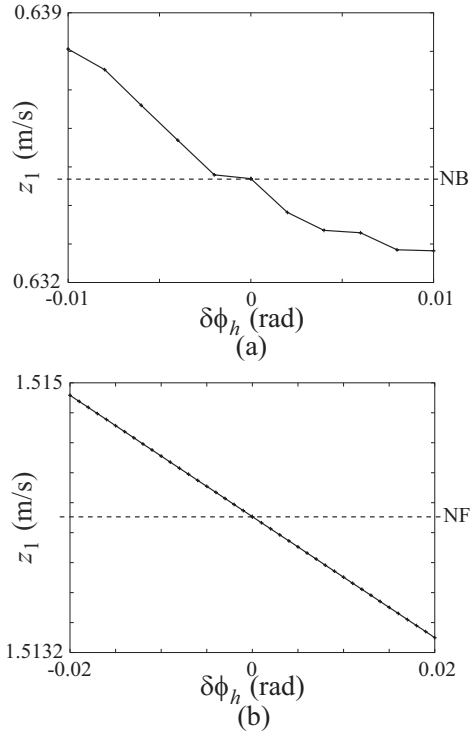

FIG. 7. (a) [(b)] Variation of z_1 at the BSP induced by a slight modulation of the posture near NB [NF]. ϕ_h is changed to $\bar{\phi}_h + \delta\phi_h$ just before the BSP at $t=t'$. For NB, $t'=2.07$ and the time of the BSP is $t=2.17$. For NF, $t'=1.817$ and the time of the BSP is $t=1.823$. Increasing $\delta\phi_h$ induces z_1 at the BSP to decrease. This result is consistent with the numerical results in Fig. 5.

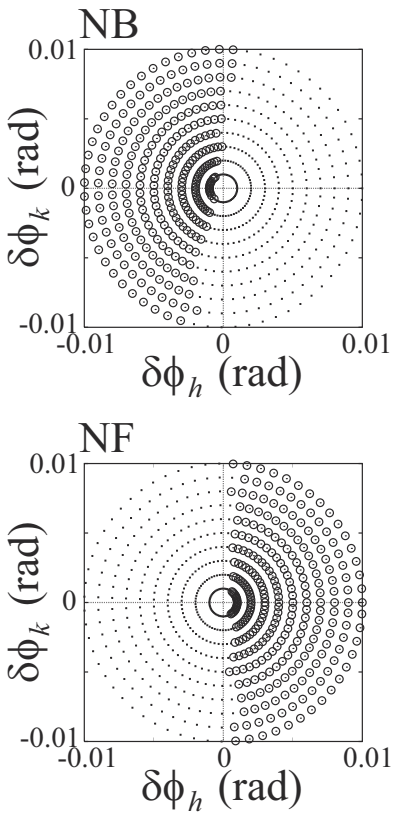

FIG. 8. (a) [(b)] Response of the system to perturbations of $\delta\phi_h$ and $\delta\phi_k$ near NB [NF] for $t_0=2.56$ [$t_0=1.82$]. The final state of the system induced by perturbation is shown, where white circles and black dots indicate the values of the parameters for which the system recovers subsequent walking or approaches a falling state, respectively.

varied appropriately for subsequent walking as shown in Fig. 8. A function f was used to control Φ_h and Φ_k when z_1 approaches Z_b or Z_f. z_b and z_f were set to 0.9 and 1.1, respectively. The signs of α_{hb}, α_{hf}, and α_{kb} were determined from the numerical results in Fig. 8. In this case $\alpha_{hb}=-0.03$, $\alpha_{hf}=0.16$, and $\alpha_{kb}=1.0$. Although, in previous sections, ϕ_h and ϕ_k in Eq. (1) were given as parameters, Eq. (2) assigns them according to the system variable (z_1). The system (2) was thus established as a complete autonomous system (Fig. 9). Hereafter we call this system the *global-variable-coordinated* (GVC) system.

Receiving the sensory signal coding for the walking velocity and the outputs from the CPG, the PC governs the leg posture around the BSP. In humans, the walking velocity could be observed by the visual cortex or through sensing the movement of the location of the peak of pressure on the foot using mechanoreceptors on the foot sole. It is known neurophysiologically that the cerebellum receives information from the visual cortex. Purkinje cells in the cerebellum also receive proprioceptive sensory signals and outputs from the CPG [21,22]. Purkinje cells in the cerebellum strongly participate in the moderate posture of the legs at the BSP. As also mentioned in Sec. II, the PC presented here may correspond to Purkinje cells in lobules IV and V of the paravermal part and the vermal zones of the cerebellum.

V. SIMULATION AND RESULTS

Using the proposed model as presented in Sec. IV (Fig. 9), the adaptability of initial-state coordination according to a global variable should be tested. Without initial-state coordination by the global variable—i.e., when the equilibrium angles of the hip and knee joints at the BSP are set to moderate fixed values—the system (1) generates a particular walking pattern. This walking pattern is similar to that generated by the model without the PC [11,12]. We call the walking movement without initial-state coordination by a global variable [$\alpha_{hf}=\alpha_{hb}=\alpha_{kb}=0$ or the model (1)] *simple walking*. The effectiveness of initial-state coordination should be demonstrated in comparison with the adaptive range of *simple walking* (Sec. III). We tested the adaptive range of the GVC system by applying various strong perturbations, while assigning fixed values to each of the equation parameters. Hereafter, we take $\theta_{in}=-0.03\pi$ rad.

A. Adaptability to external forces

The GVC system was tested in the case that an unpredictable and temporary external force is applied. It was assumed that an external force takes effect on the hip in the horizontal direction over a 0.1-s interval during walking. This perturbation may, for example, correspond to collision with an oncoming human.

The maximum force that may be applied to the walking system depends on the gait phase at which the perturbation is

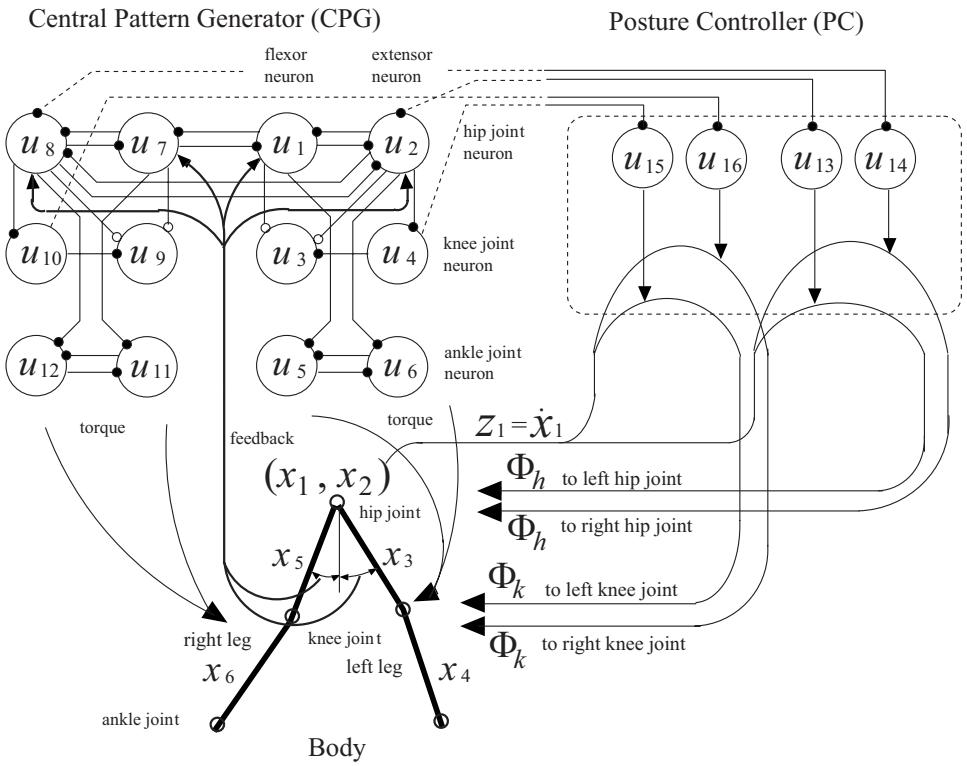

FIG. 9. A conceptual control diagram of the proposed model. According to z_1, the PC determines the equilibrium angles Φ_h and Φ_k for posture modulation at BSP. Assigning the equilibrium angles Φ_h and Φ_k, the PC modulates the angles of the hip and knee joints, respectively.

applied [25]. Figure 10(a) shows the maximum force that may be applied to the GVC system and to the simple walking model as a function of the gait phase corresponding to the moment the external force was applied. The gait phase is measured from the BSP of the left leg (it is 0 at the BSP of the left leg). Positive and negative forces indicate forward and backward forces, respectively. The GVC system could overcome forces greater than 400 N in any gait phase. Figures 10(b) and 10(c) show stick figures representing the walking patterns of the simple model and the GVC system when a forward force of 400 N was applied at gait phase $3\pi/4$. Figure 10(d) shows a time series of the walking velocity z_1 and the hip and knee joint angles on one side during the walking movement shown in Fig. 10(c). The modulation of the hip and knee joint angle at the BSP depends on the walking velocity z_1; i.e., initial-state coordination enabled the walking system to adapt to large temporary forces.

The next test of the model involved the case when an external force is applied continuously. It was assumed that an external force has a continuous effect with a constant strength on the hip in the horizontal direction during walking. This may resemble the situation when a walking human is buffeted by a gust of wind—e.g., when cities are visited by a typhoon or a hurricane. Although the range of such forces that can be applied to simple walking is from −17 N (backward force) to 42 N (forward force), the GVC system considerably extends this range to −40 N (backward force) and 107 N (forward force). Figures 11(a)–11(d) show stick figures expressing the walking motion when such forces are applied. Figures 11(e) and 11(f) indicate the time series of the walking velocity z_1 and the hip and knee joint angles on the one side during the walks shown in Figs. 11(b) and 11(d), respectively. Initial-state coordination could therefore enable the walking system to adapt to strong continuous forces.

The GVC system overcomes perturbations by forming the leg posture at the BSP. That is, the strategy applies a load to the hip and knee joints at the BSP. However, as described in (1), the model does not produce a torque amplitude in excess of δ_h and δ_k at the hip and knee joints, respectively. The parameters δ_h and δ_k were set to 100 Nm and 70 Nm, respectively. The adaptive strategy could therefore be realized with hip and knee joint torque amplitudes within 0.14 and 0.1 (torque [Nm]/weight [N]), since the assumed bodyweight is 70 kg≅700 N. This torque amplitude is equal to that during normal human walking as shown in biomechanical studies [20]. Therefore, the adaptive strategy is considered to be appropriate in terms of torque level. As an example, Fig. 10(e) shows the time series of the active torque generated at the hip and knee joints during the adaptive walking movement.

B. Adaptability to impairment

During walking, the foot develops the propulsive force needed to move the body forward through interaction with the ground. The ankle joint torque plays a decisive role in the development of this propulsive force [26]. Restricting the ankle joint torque level should therefore penalize walking performance heavily. However, even when the ankle joint(s) are rendered immobile through injury, humans can usually walk.

We considered such a case, supposing that the torque level of the ankle joint(s) (α_l and α_r in Appendix A) suddenly becomes zero during walking. It was confirmed that during simple walking (without initial-state coordination by z_1) even the impairment of one ankle joint makes the walking system fall, as shown in Fig. 12(a). On the other hand, the GVC system enables the system to overcome the impairment. The solution orbit approaches a different quasiperiodic

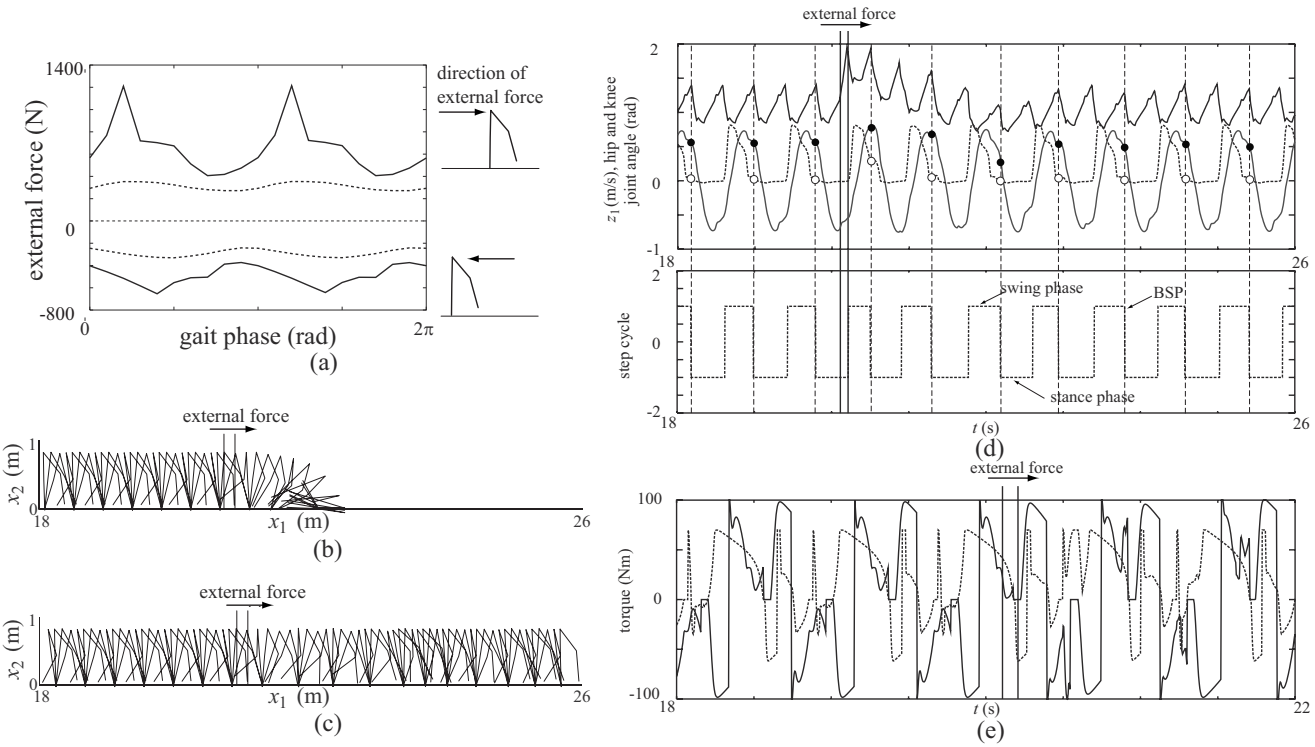

FIG. 10. (a) Adaptability of the GVC system to a temporary external force applied to the hip in the horizontal direction over a 0.1-s interval during walking. Solid (dashed) lines indicate the maximum force that could be applied to the GVC system (simple walking). The arithmetic sign of the force indicates a forward or backward direction in the force vector. The x axis indicates the gait phase when the external force is applied. The gait phase is measured from the BSP (it is 0 at the BSP). (b) and (c) show stick figures for simple walking and the GVC system, respectively, when a forward external force of +400 N acts at gait phase $3\pi/4$ shown in (a). The two tall vertical lines indicate the interval of 0.1 s during which the force acts. (d) Motion of variables in the walking movement shown in (c). The time series of z_1 (solid line), the angle of the left hip joint, x_3-x_5 (gray line), the angle of the left knee joint, x_3-x_4 (dashed line), and the step cycle (the stance and swing phase) of the left leg (dotted line) are indicated. ● and ○ denote the angles of the hip and knee joints, respectively, at the BSP. The hip (●) and knee joint angles (○) at the BSP were modulated according to the value of z_1 (solid line), which led to successful overcoming of the perturbation. (e) The time series of the total active torque generated at the left hip (solid line) and knee joint (dashed line) are indicated. This shows that the adaptive motion is generated using joint torques within the normal torque level.

orbit from that before impairment. The model could continue to walk under such a sudden impairment of a single ankle joint. Figure 12(b) shows a stick figure representing a motion of the GVC system when the left ankle joint is suddenly impaired.

Even when the ankle joint is impaired, humans can begin walking from a standing position and achieve stable walking. The transition from a standing position to stable walking is referred to here as the initiation process. Regarding the condition of sudden impairment discussed above, the strategy has already been demonstrated capable of overcoming it using model (1) where ϕ_h and ϕ_k were taken as constants in the model, but ϕ_k was abruptly shifted to another constant value in accordance with a change in the ankle torque levels α_l and α_r [12]. We tested whether the strategy achieved the initiation process under ankle joint impairment. Regarding the initiation process, the model is equivalent to (1) since ϕ_k is fixed from $t=0$ to reflect the impairment. By investigating the parameter settings, we found that the model cannot establish subsequent walking for any θ_{in} and ϕ_k. This indicates that the strategy adopted in [12] cannot achieve the initiation process.

On the other hand, the GVC system is capable of achieving the initiation process. Figures 12(c) and 12(d) show stick figures representing the walking motion from the initiation process to stable walking with the ankle joint impaired on only one leg and on both legs, respectively. The initial-state coordination by the global variable was thus shown to enable the impaired system to achieve the initiation process.

VI. DISCUSSION

Taga [25,27] modeled a human walking system by using the "global angular velocity" which indicates the angular velocity of the vector from the body's center of gravity to the center of pressure due to the ground reaction force. This variable may play a similar role to the global variable presented here. Taga's model has demonstrated adaptability to environmental and task conditions. Taga integrated it into the entrainment from the body to the CPG and utilized it for the stabilization of the mutual entrainment. In a sense, this restricts the function of the global variable to the stabilization of the basic gait pattern. The model responds to perturbations by producing joint torques at an amplitude corresponding to that of the global variable. This means that this global variable has been dealt with at the same level as other variables expressing the motion of the system components, such as

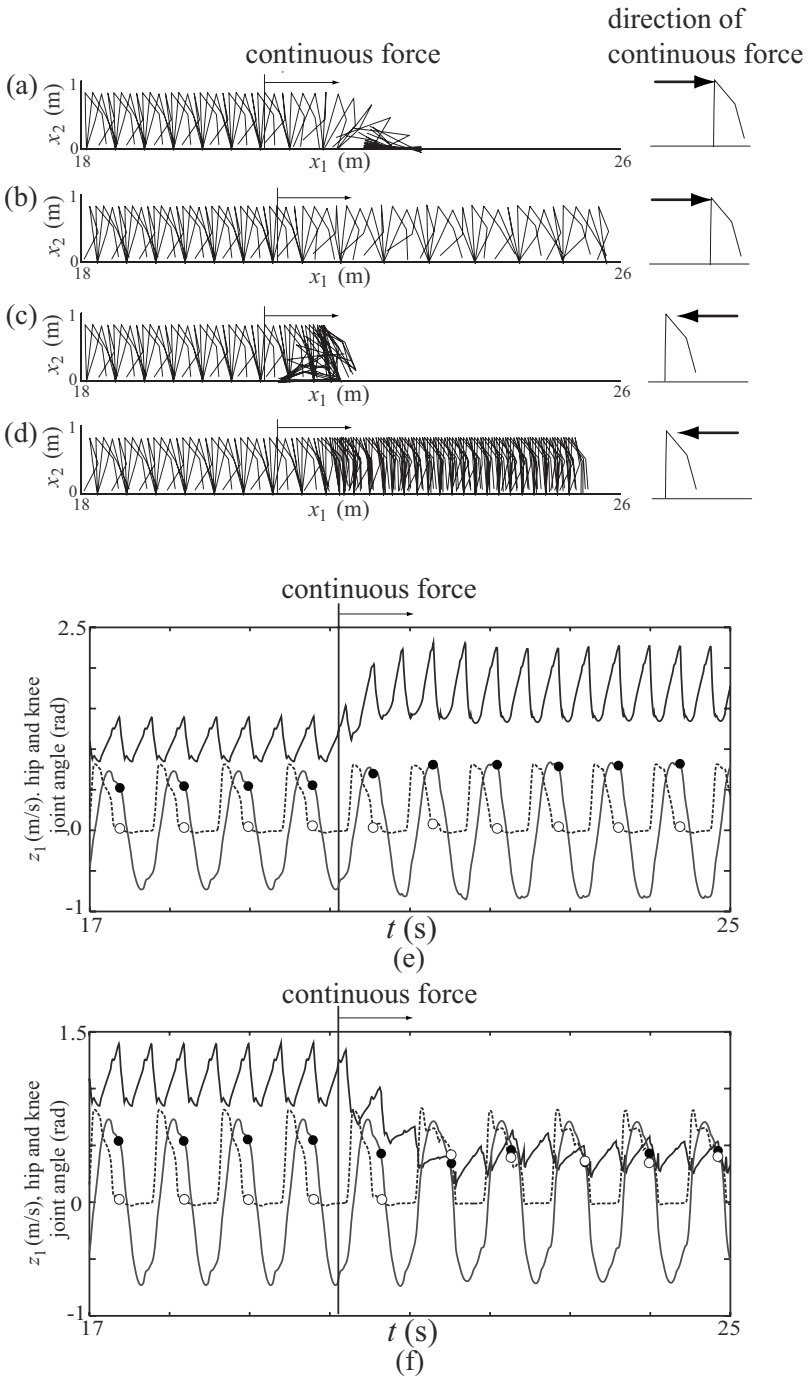

FIG. 11. (a) and (b) show stick figure for simple walking simulation and a walking simulation based on the GVC system, respectively, when an external forward force of +100 N acts on the hip continuously. The tall vertical line indicates the time at which the perturbation begins. (c) and (d) show a simple walking simulation and a walking simulation based on the GVC system, respectively, when an external backward force of −40 N acts on the hip continuously. (e) and (f) Motion of variables during walking movements shown in (b) and (d), respectively. The time series of z_1 (solid line), the angle of the left hip joint, x_3-x_5 (gray line), and the angle of the left knee joint, x_3-x_4 (dashed line), of the left leg are indicated. ● and ○ denote the angle of the hip and knee joints, respectively, at the BSP. This information shows that the hip (gray line) and knee joint angles (dashed line) at the BSP were modulated according to the value of z_1 (solid line), which led to successfully overcoming the perturbation.

joint motion and neuronal firing. In contrast, we have provided numerical proof that the instant velocity of hip position (z_1) is a global variable. In the GVC system, which induces control of the leg posture near the neutral state (at the BSP), the global variable z_1 is used only to control which basin the system is attracted to. The GVC system responds to perturbations by modulating the leg posture [δ_h and δ_k in (1)] within the torque level of normal walking.

Focused on trajectories of a walking system following a Poincaré section, studies in robotics have developed methods for recovering the original stable trajectory following perturbations and demonstrated the reliability of the recoveries' effectiveness using a stability analysis [28–30] and delayed feedback control approach [10,31]. The GVC system is designed so that the initial state is located somewhere inside the particular attractor basin by encoding the attractor basins near neutral states. Although bipedal walking models that are adaptive to strong perturbations have been discussed in [12,25,27–34], an autonomous adaptive model which reproduces human walking adaptability to both physical and environmental perturbations has not been proposed.

From a mathematical viewpoint, a hierarchy is the structure according to which the low-dimensional dynamics of a small number of variables can govern the dynamics of a large number of degrees of freedom over a whole system. A small set of variables and a collection of other variables are

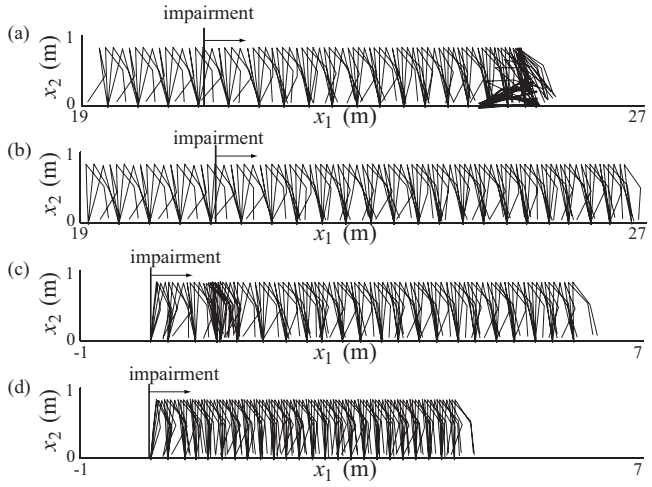

FIG. 12. Adaptability of the GVC system to impairment conditions in the ankle joint(s). (a) and (b) Stick figures representing simple walking and the GVC system's walking, respectively, for the case when the torque acting at one ankle joint suddenly becomes 0 during walking. The vertical line indicates the timing at which the change occurs. (c) and (d) Impairments applied from the onset of walking; i.e., the torque level of the ankle joint(s) is 0 from the beginning and throughout walking. (c) and (d) show stick figures representing walking motion of the GVC system in the case that the impairment condition is applied to one leg and both the legs, respectively. Numerical simulation more than 100 s shows walking of the GVC system with impairment(s), i.e., in (b), (c), and (d), to be stable in the corresponding time interval.

referred to as the higher and lower levels, respectively. When the fate of the solution orbit of the system is determined by a small number of variables, and other variables are in turn governed by them, the system can be considered to be hierarchical.

In this paper, we define a global variable as dominant directions in the dynamics of the system near neutral states. Numerical experiments near neutral states revealed the following.

(I) The walking velocity z_1 is a global variable and can dominate other variables near neutral states.

(II) The posture at the BSP is the initial state, and it determines which attractor basin the system belongs to.

These findings ensure that the dynamics of the system with its large number of degrees of freedom can be governed by the one-dimensional dynamics of the global variable z_1 near the neutral states if the initial state is coordinated by this global variable. The equations coordinating the initial state by the global variable were constructed accordingly. The walking system was thus constructed hierarchically and consists of two levels including the global and other variables.

By using oscillator models, theoretical studies of human locomotion [35,36] have indicated that the walking speed is an important parameter in determining walking patterns. Moreover, it has been shown in [35] that walking pattern transitions dependent on the walking speed are biomechanically appropriate with respect to energy cost. We note that in this article the relationship between walking speed, energy cost, and hierarchy structure among all the variables, including the neural system, has not been clarified.

Regarding the hierarchy, we emphasize the following point. The hierarchic structure proposed here is different from that of a master-slave relationship such as the slaving principle [19], because in the GVC system the interaction between the two levels is clearly active only when the system draws near to neutral states. In other states of the system such as stable walking states, the global variables or elements in hierarchically higher levels are not crucial for the walking dynamics because Φ_h and Φ_k are not affected by the global variables for $z_b \leq z_1 \leq z_f$. Indeed, in a stable walking state, a walking motion trajectory generated by the system is similar to a trajectory generated by simple walking in which coordination functions based on a global variable are not integrated (without the PC). We have shown that such an "instability-induced hierarchy" can yield flexibility.

APPENDIX A: THE EQUATIONS OF BODY MOTION AND CPG

All variables and conventions correspond to those shown in Fig. 2. By using the Newton-Euler method used in [4], the motion of the body can be written as follows:

$$P(\mathbf{x})\ddot{\mathbf{x}} = \mathbf{Q}(\mathbf{x},\dot{\mathbf{x}},\mathbf{T}(\mathbf{u},\mathbf{x},\dot{\mathbf{x}}),\mathbf{T}_{BSP}(\mathbf{u},\mathbf{x}),\mathbf{F}), \tag{A1}$$

and therefore,

$$\ddot{\mathbf{x}} = [P(\mathbf{x})]^{-1}\mathbf{Q}(\mathbf{x},\dot{\mathbf{x}},\mathbf{T}_r(\mathbf{u},\mathbf{x},\dot{\mathbf{x}}),\mathbf{T}_{BSP}(\mathbf{u},\mathbf{x}),\mathbf{F}),$$

where an overdot denotes the derivative with respect to t,

$$\mathbf{x} = (x_1,x_2,x_3,x_4,x_5,x_6)^{\mathrm{T}},$$

$$\mathbf{Q}(\mathbf{x},\dot{\mathbf{x}},\mathbf{T}_r(\mathbf{u}),\mathbf{T}_{BSP}(\mathbf{u},\mathbf{x}),\mathbf{F}) = (q_1,q_2,q_3,q_4,q_5,q_6)^{\mathrm{T}},$$

$$\mathbf{T}_r(\mathbf{u},\mathbf{x},\dot{\mathbf{x}}) = (T_{r1},T_{r2},T_{r3},T_{r4},T_{r5},T_{r6})^{\mathrm{T}},$$

$$\mathbf{F} = (F_1,F_2,F_3,F_4,F_5,F_6)^{\mathrm{T}},$$

and the 6×6 real matrix $P(\mathbf{x})$ is same as that in [12],

$$q_1 = (0.5m_2 + m_3)l_1 \sin(x_3)\dot{x}_3^2 + 0.5m_3l_2 \sin(x_4)\dot{x}_4^2 + (0.5m_4 + m_5)l_3 \sin(x_5)\dot{x}_5^2 + 0.5m_5l_4 \sin(x_6)\dot{x}_6^2 + F_{g1} + F_{g3} + F_1,$$

$$q_2 = -(0.5m_2 + m_3)l_1 \cos(x_3)\dot{x}_3^2 - 0.5m_3l_2 \cos(x_4)\dot{x}_4^2 - (0.5m_4 + m_5)l_3 \cos(x_5)\dot{x}_5^2 - 0.5m_5l_4 \cos(x_6)\dot{x}_6^2 + F_{g1} + F_{g2} - \sum_{n=1}^{5} m_n g + F_2,$$

$$q_3 = 0.5m_3l_1l_2 \sin(x_4 - x_3)\dot{x}_4^2 - (m_2 + 2m_3)0.5gl_1 \sin(x_3) + F_{g1}l_1 \cos(x_3) + F_{g2}l_1 \sin(x_3) + T_{rp1} + T_{r1} - T_{r2} - T_{r4} - T_{BSPl} + F_3,$$

$$q_4 = 0.5m_3l_1l_2 \sin(x_3 - x_4)\dot{x}_3^2 - 0.5m_2gl_2 \sin(x_4) + F_{g1}l_2 \cos(x_4) + F_{g2}l_2 \sin(x_4) + T_{rp2} + T_{r2} - T_{r3} + T_{BSPl} + F_4,$$

$$q_5 = 0.5m_5l_3l_4\sin(x_6 - x_5)\dot{x}_6^2 - 0.5(m_4 + 2m_5)gl_3\sin(x_5) + F_{g3}l_3\cos(x_5) + F_{g4}l_3\sin(x_5) + T_{rp3} + T_{r4} - T_{r5} - T_{r1} - T_{BSPr} + F_5,$$

$$q_6 = 0.5m_5l_3l_4\sin(x_5 - x_6)\dot{x}_5^2 - 0.5m_4gl_4\sin(x_6) + F_{g3}l_4\cos(x_6) + F_{g4}I_4\sin(x_6) + T_{rp4} + T_{r5} - T_{r6} + T_{BSPr} + F_6.$$

F_{gi} $(i=1,\ldots,4)$ are the horizontal and vertical forces on the ankles (see detail in [12]).

Passively generated torques at each joint are given by

$$T_{rp1} = k_r f(x_4 - x_3) - b_r f(x_4 - x_3) - b_0(\dot{x}_3 - \dot{x}_5) - b_0(\dot{x}_3 - \dot{x}_4),$$

$$T_{rp2} = -k_r f(x_4 - x_3) + b_r f(x_4 - x_3) - b_0(\dot{x}_4 - \dot{x}_3) - b_0\dot{x}_4,$$

$$T_{rp3} = k_r f(x_6 - x_5) - b_r f(x_6 - x_5) - b_0(\dot{x}_5 - \dot{x}_3) - b_0(\dot{x}_5 - \dot{x}_6),$$

$$T_{rp4} = -k_r f(x_6 - x_5) + b_r f(x_6 - x_5) - b_0(\dot{x}_6 - \dot{x}_5) - b_0\dot{x}_6,$$

where k and b are positive constants.

Actively generated torques at each joint are given by

$$T_{r1} = p_1 f(u_1) - p_2 f(u_2) + T_{BSPlh} - T_{BSPrh},$$

$$T_{r2} = p_3 f(u_2) - p_4 f(u_4) + T_{BSPlk} + T_{rl},$$

$$T_{r3} = \alpha_l[p_5 f(u_5) - p_6 f(u_6)]g(-y_l) - T_{BSPlk} - T_{rl},$$

$$T_{r4} = p_1 f(u_7) - p_2 f(u_8) - T_{BSPlh} + T_{BSPrh},$$

$$T_{r5} = p_3 f(u_9) - p_4 f(u_{10}) + T_{BSPrk} + T_{rr},$$

$$T_{r6} = \alpha_r[p_5 f(u_{11}) - p_6 f(u_{12})]g(-y_r) - T_{BSPrk} - T_{rr},$$

$$T_{rl} = g(u_1)\{-p_7[f(x_3 - x_4 - x_k)]^2 - p_8(\dot{x}_3 - \dot{x}_4)\},$$

$$T_{rr} = g(u_7)\{-p_7[f(x_5 - x_6 - x_k)]^2 - p_8(\dot{x}_5 - \dot{x}_6)\},$$

where α_l and α_r are parameters expressing the ankle joint torque in the left and right legs, respectively. The values of α_l and α_r are set to 0 and 1 for the normal and impaired situations, respectively. T_{rl} and T_{rr} are voluntary control torques which roughly restrict the maximum flection angle of the left and right knee joints to a positive constant x_k rad during each swing phase. The other equations and parameters used in the model presented here and those in the previous model [12] are identical.

The neural system is represented by the following differential equations [37]:

$$\tau_i\dot{u}_i(t) = u_i(t) - v_i(t) - u_i(t)^3/3 + \sum_{j=1}^{16} w_{ij}f(u_j(t)) + u_0 + E_i(\mathbf{x}(t)),$$

$$\tau_i'\dot{v}_i(t) = u_i(t) + a - bv_i(t),$$

$$E_1 = E_8 = -E_2 = -E_7 = f(-x_3) - f(-x_5),$$

$$E_i = 0 \quad \text{(otherwise)},$$

$$f(u_i) = \max(0, u_i) \quad (i = 1, \ldots, 16),$$

where u_i is the potential of the ith neuron and v_i is responsible for the accommodation and refractoriness of the ith neuron.

APPENDIX B: SIMULATION PARAMETERS

1. Body

The parameters for the body are

$$m_1 = 48.0 \text{ kg}, \quad m_2 = m_4 = 7.0 \text{ kg}, \quad m_3 = m_5 = 4.0 \text{ kg},$$

$$l_1 = l_3 = 0.4 \text{ m}, \quad l_2 = l_4 = 0.45 \text{ m},$$

$$I_i = m_{i+1}l_i^2/12 \text{ kg m}^2 \quad (i = 1,2,3,4),$$

$$k_g = 30000.0 \text{ kg/s}^2, \quad k_r = 2000.0 \text{ kg/s}^2,$$

$$b_g = 3000.0 \text{ kg/s}, \quad b_r = 200.0 \text{ kg/s}^2, \quad b_0 = 1.0 \text{ kg/s},$$

$$p_1 = p_2 = p_4 = 24.0 \text{ kg rad s}^{-2} \text{ mV}^{-1},$$

$$p_3 = 31.2 \text{ kg rad s}^{-2} \text{ mV}^{-1},$$

$$p_5 = 20.0 \text{ kg rad s}^{-2} \text{ mV}^{-1},$$

$$p_6 = 0.0 \text{ kg rad s}^{-2} \text{ mV}^{-1},$$

$$p_7 = 400.0 \text{ kg rad s}^{-2} \text{ mV}^{-1},$$

$$p_8 = 40.0 \text{ kg rad s}^{-2} \text{ mV}^{-1},$$

$$\beta_h = \beta_k = 50.0 \text{ kg rad s}^{-2} \text{ mV}^{-1},$$

$$p_{h1} = p_{k1} = 500.0 \text{ kg rad s}^{-2} \text{ mV}^{-1},$$

$$p_{h2} = p_{k2} = 50.0 \text{ kg rad s}^{-2} \text{ mV}^{-1},$$

$$\delta_h = 100.0 \text{ kg rad}^2 \text{ s}^{-2}, \quad \delta_k = 70.0 \text{ kg rad}^2 \text{ s}^{-2},$$

$$x_k = 0.2\pi \text{ rad}, \quad g = 9.8 \text{ ms}^{-2},$$

$$\phi_h = 0.13\pi \text{ rad}, \quad \phi_k = 0.01 \ \pi \text{ rad}.$$

2. Neural system (central pattern generator and posture controller)

The paramters for the neural system are

$$\tau_4 = \tau_{10} = \tau_{13} = \tau_{14} = 1/50,$$

$$\tau_i = 1/30 \quad \text{(otherwise)},$$

$$\tau'_4 = \tau'_{10} = \tau'_{13} = \tau'_{14} = 20/3,$$

$$\tau_i = 10/3 \quad \text{(otherwise)},$$

$$u_0 = 0.3, \quad a = 0.7, \quad b = 0.8,$$

$$w_{1\ 5} = w_{2\ 6} = w_{2\ 4} = w_{4\ 3} = -1.0,$$

$$w_{5\ 6} = w_{6\ 5} = w_{1\ 7} = w_{7\ 1} = -1.0,$$

$$w_{7\ 12} = w_{8\ 12} = w_{8\ 10} = w_{10\ 9} = -1.0,$$

$$w_{11\ 12} = w_{12\ 11} = w_{2\ 8} = w_{8\ 2} = -1.0,$$

$$w_{4\ p1} = w_{10\ p2} = -1.0,$$

$$w_{1\ 2} = w_{2\ 1} = w_{7\ 8} = w_{8\ 7} = -2.0,$$

$$w_{1\ 3} = w_{2\ 3} = w_{7\ 9} = w_{8\ 9} = 1.0,$$

$$w_{ij} = 0.0 \quad \text{(otherwise)}.$$

3. Initial conditions

The parameters for the initial conditions are

$$x_1 = 0.0 \text{ m}, \quad x_2 = (l_1 + l_2)\cos\theta_{in} \text{ m},$$

$$x_3 = x_4 = x_5 = x_6 = \theta_{in} \text{ rad},$$

$$\dot{x}_i = 0 \quad (i = 1, \ldots, 6),$$

$$u_i = -0.199408 \text{ mV} \quad \text{for} \quad i = 1, 8, 13,$$

$$u_i = -1.199408 \text{ mV} \quad \text{(otherwise)},$$

$$v_i = -0.624260 \quad (i = 1, \ldots, 16).$$

[1] J. B. Dingwell and J. P. Cusumano, Chaos **10**, 848 (2000).
[2] F. El-Hafi and P. Gorce, in *Proceedings of the 1998 IEEE International Conference on Systems, Man, and Cybernetics* (IEEE, New York, 1998), p. 3538.
[3] G. Taga, Physica D **75**, 190 (1994).
[4] G. Taga, Y. Yamaguchi, and H. Shimizu, Biol. Cybern. **65**, 147 (1991).
[5] S. Grillner, Science **228**, 143 (1985).
[6] B. Calancie, B. Needham-Shropshire, P. Jacobs, K. Willer, G. Zych, and B. Green, Brain **117**, 1143 (1994).
[7] M. Dimitrijevic, Y. Gerasimenko, and M. Pinter, Ann. N.Y. Acad. Sci. **860**, 360 (1998).
[8] T. Teramoto, K.-I. Ueda, and Y. Nishiura, Phys. Rev. E **69**, 056224 (2004).
[9] T. Teramoto, K.-I. Ueda, and Y. Nishiura, Prog. Theor. Phys. Suppl. **161**, 364 (2006).
[10] B. R. Andrievskii and A. L. Fradkov, Autom. Remote Control (Engl. Transl.) **64**, 673 (2003).
[11] A. Ohgane, K. Ohgane, H. Mahara, and T. Ohtsuki, Forma **19**, 427 (2004).
[12] A. Ohgane, K. Ohgane, S. Ei, H. Mahara, and T. Ohtsuki, Biol. Cybern. **93**, 426 (2005).
[13] M. Udo, K. Matsukawa, and H. Kamei, Brain Res. **160**, 559 (1979).
[14] M. Udo, K. Matsukawa, H. Kamei, and Y. Oda, J. Neurophysiol. **44**, 119 (1980).
[15] D. M. Armstrong and S. A. Edgley, J. Physiol. **352**, 403 (1984).
[16] M. Udo, K. Matsukawa, H. Kamei, K. Minoda, and Y. Oda, Exp. Brain Res. **41**, 292 (1981).
[17] M. Udo, Y. Oda, K. Tanaka, and J. Horikawa, Prog. Brain Res. **44**, 445 (1976).
[18] W. W. Chambers and J. M. Sprague, AMA Arch. Neurol. Psychiatry **74**, 653 (1955).
[19] H. Haken, *Advanced Synagetics: Instability Hierarchies of Self-Organizing Systems and Devices* (Springer-Verlag, Berlin, 1983).
[20] H. Elfman, Am. J. Physiol. **125**, 339 (1939).
[21] Y. I. Arshavsky, I. M. Gelfand, and G. N. Orlovsky, Trends Neurosci. **6**, 417 (1983).
[22] M. Ito, *The Cerebellum and Neural Control* (Raven, New York, 1994).
[23] S. Rietdyk, Gait Posture **23**, 268 (2006).
[24] J. Perry, *Gait Analysis: Normal and pathological function* (SLACK, Thorofare, NJ, 1992).
[25] G. Taga, Biol. Cybern. **73**, 113 (1995).
[26] D. A. Winter, *Biomechanics and Motor Control of Human Movement*, 2nd ed. (Wiley, New York, 1990).
[27] G. Taga, Biol. Cybern. **73**, 97 (1995).
[28] C. Chevallereau, E. R. Westervelt, and J. W. Grizzle, Int. J. Robot. Res. **24**, 431 (2005).
[29] J. W. Grizzle, G. Abba, and F. Plestan, IEEE Trans. Autom. Control **46**, 51 (2001).
[30] H. Ye, A. N. Michel, and L. Hou, IEEE Trans. Autom. Control **43**, 461 (1998).
[31] Y. Sugimoto and K. Osuka, in *Proceedings of the IEEE International Conference on Robotics and Biomimetics* (IEEE, New York, 2004), p. 606.
[32] G. Taga, Biol. Cybern. **78**, 9 (1998).
[33] T. Yamasaki, T. Nomura, and S. Sato, Biol. Cybern. **88**, 468 (2003).
[34] A. Ishiguro, A. Fujii, and P. Eggenberger, Adapt. Behav. **11**, 7 (2003).
[35] V. B. Kokshenev, Phys. Rev. Lett. **93**, 208101 (2004).
[36] B. J. West and N. Scafetta, Phys. Rev. E **67**, 051917 (2003).
[37] R. Fitzhugh, Biophys. J. **1**, 445 (1961).